Indian Journal of Natural Sciences www.tnsroindia.org.in ©IJONS

Vol.9 /Issue 52 / February / 2019 *International Bimonthly* *ISSN: 0976 – 0997*

RESEARCH ARTICLE

Using Dual Polarimetric SAR Data to Investigate the Cultural Heritage Remnants in Ukhaidir Fortress Southwest Karbala City, Iraq

Zaidoon Taha Abdulrazzaq[1*] Jassim Muhammad Thabit[2] and Ammar Jasim Al-Khafaji[3]

[1]Directorate of Space and Communications, Ministry of Science and Technology, Baghdad, Iraq
[2]Department of Geology, College of Science, University of Baghdad, Baghdad, Iraq
[3]Department of Biology, College of Science, University of Karbala, Karbala, Iraq

Received: 21 Nov 2018 Revised: 25 Dec 2018 Accepted: 27 Jan 2019

[*]**Address for Correspondence**
Zaidoon Taha Abdulrazzaq
Directorate of Space and Communications,
Ministry of Science and Technology,
Baghdad, Iraq.
Email: zaidoon.taha@live.com

ABSTRACT

Iraq is one of the countries that contain many important archaeological sites and manifestations of varied cultural heritage belonging to ancient civilizations, and several archaeological sites and cultural heritage are disappeared as a result of neglect. In this study, Synthetic Aperture Radar data was used to extract information regarding potential archaeological remains in Ukhaidir site, southwest of Karbala city, which is considered to be a good and new contribution in the field of archaeological sensors utility applied by space-borne radar. ALOS PALSAR (L-band) image was used to identify and detect the ground anomalies due to the presence of near-surface archaeological structures. Advanced image processing and classification were applied depending on the intensity bands (HH and HV) including texture analysis by application of the GLCM algorithm and unsupervised classification using the K-means algorithm to nominate potential archaeological sites. The results led us to identify twelve sites, seven of them were excluded because they were not covered and clearly visible in the recent high-resolution image and in the field observation, which appears as hills containing scattered stone remains and brick walls. The five sites nominated (P1, P2, P3, P4 and P5), were completely covered with loose sand, and its areas are ranging between 873-3774 km^2 approximately. The sites P1 and P2 are located northeast of the fortress and P4 and P5 sites in the southwest, while P3 is located about 380 m in the southeast. Potentially, they might be represented remains of structures for houses or rooms used for military purposes or secret caches connected to the fortress through tunnels.

Keywords: ALOS PALSAR,Texture analysis, Clustering,Potential archaeological sites.

INTRODUCTION

During the last century, the techniques of Remote Sensing (RS) have proven to be a powerful tool and a great potential in archaeological prospecting [1-4]. The use of RS techniques have an honorable history in archaeological studies by utilizing space-borne sensors, where it showed its potential at the end of 1800.It is characterized by being able to estimate and calculate surface and subsurface parameters without direct contact. This is considered of great importance in archaeological surveys because they are non-destructive techniques[5,6]. However, RS techniques are usually used in combination with other methods in archaeological investigation such as geophysical methods and Geographic Information System (GIS) as well as collecting historical information about the site by traditional methods. Synthetic Aperture Radar (SAR) data in the early 1980s showed capabilities in archaeological studies, especially after the availability of spatial resolutions better than 30 meters. Moreover, long-wavelength radar data in arid environments are capable of penetrating the surface of soil and loose sand to near-surface targets[7-11].Another useful feature is the backscatter from SAR instruments which depends on the soil moisture [12], surface roughness [13], the incidence angle [14], the geometry of targets [15],the frequency and polarization [16], these properties may be suitable to detect various features of buried archaeological structures. The depth of penetration of SAR is based on the wavelength and frequency of the sensor in addition to the conductivity and dielectric permittivity of soil[17-19],where the penetration depth decreases with increasing frequency of the sensor and soil moisture content during the capture time.

The possibility of discerning and detecting of the buried archaeological remains, in addition to the availability of multi-platform with high-resolution data, encouraged the scientists' community to use orientation space-borne SAR data in this field[20]. Among space platforms so far released, ALOS PALSAR (advanced land observing satellite phased array type L-band synthetic aperture radar) of 1.27 GHz center frequency is one of the best SARs used in the field of archaeological investigation[21]. Due to the availability of high-resolution (up to 10 m), multi-temporal and polarimetric archival data, many researchers have used ALOS PALSAR in this fieldlike [20-25].In spite of the development of modern technology and software with the availability of good quality data, the processing and interpretation of SAR data is still complex and also relies on the nature of the site of study. Therefore, the choice of the appropriate location is the first stage of interpretation. It is preferable to be within a geographical area with appropriate climatic conditions, large enough for the spatial resolution and located within the elevated area of sediments and not previously flooded, in addition to its historical and cultural significance.

The identification of the buried archaeological structures,based on SAR data is insufficient as these structures cannot be distinguished if they are buried or visible on the surface. Thus, it is necessary to use another type of data have featured surface images for comparison and illustration[22]. The aim of the current study, in light of previous investigations and excavations at the site of Ukhaidir, is to follow an approach that includes the processing and interpretation of ALOS image based on the texture analysis of the intensity of HH and HV bands, and to compare the results with the present high-resolution image, 3D image view andthe field observations to ensure that the potential archaeological structures are fully covered.Finally,the selecting of potential archaeological sites and the excavation at these potential sites lead us to new discovery sites, which contributes to the identification of the constructor of the fortress and its lost history.

THE STUDY AREA

Site Description

Ukhaidir is the name of the enormous ancient fortress which is still existing so far in a historically great location situated between latitudes 32° 25'-32° 26' North, and longitudes 43° 35'-43° 36' East as shown in Figure 1. At this location, trade caravan routes were meeting, joining Iraq to the Arabian Gulf, Arab Sea and the Mediterranean Sea

and Aleppo, and rest stops were established for passengers and trade caravans at different distances. Ukhaidir fortress locates 50 km southwest the city of Karbala and around 192 km southwest of Baghdad[26]. The fortress is surrounded by a great solid wall with a height of nearly 21 m built in the shape of a rectangle with sides of 175 x 169 m, and in the middle of each four sides, there is a wide entrance. On each of the four corners of the wall, there is a round tower of 5 m diameter. Currently, the wall is 17 m high and about 4.50 m thick. On the top of the wall, there are vertical and horizontal turrets to shoot arrows and throw fire on enemies[27]. An outer adobe-brick wall also surrounds the fortress, supported by semicircular towers from its four sides to repulse the enemy attacks [28]. The climate of the region is considered an arid climate (Desert climate), which includes a hot dry summer and cold dry winter. Topographically, the fortress is located at a height of 38 m above sea level, surrounded by a simple topography, with gentle slope terrain oriented to the northeast toward Wadi Al-Abyadh (white valley).

Archaeological History

The Mesopotamian architecture was clearly of interest and focus of many researchers and archaeologists, especially Ukhaidir fortress. They differed in determining the date of its construction and by whom it was constructed. Most studies referred to that it was constructed at the outset of Abbasid Caliphate, most likely in the era of second Abbasid caliph Al Mansoor Billah (754 – 775 AD). Bell's article in 1910 [29]was the first published on the site of Ukhaidir, which attempted to describe and date this remarkable structure[30]. As some thought, it is dated back to Sasanian period according to the shape of ancient arches and vaults which are similar to the great arch of the Taq-iKisra (The famous arch of Ctesiphon), it is one of the earliest surviving examples employing simple brickwork designs inside a series of horizontally aligned blind arches[31,32].In addition, the arches present at Ukhaidir fortress confirm that it must be Islamic in the era of Umayyad or Abbasid [33], where it was noted that the width of the arch and opening were smaller than the width of the arch of the Sasanian period[30]. On the other hand, the fortress has a similar arrangement of Qasr-iShirin in the palace of KhusrauParvèz (590-628 AD) were Iwan and its flanking chambers have become much deeper, and in the front of them is a portico of three arches and where passages at the side lead into a court at the back. The analogy is so great that one could recognize that the Abbasids followed the Sasanian tradition [34]. Herzfeld believed that it was constructed about 21s AH (890 AD) depending on the similarity between Ukhaidir and the edifices of Abbasid Samarra, whereas Bell [35],tended to believe that it was situated at the location (Dogat Al-Hira) near AinTamir which was built by the Arab prince Al-Yazeed Bin Abdulmalik, i.e. within the Umayyad Era.

In order to determine the exact date of the fortress, the Atomic Radiation Test of Carbon 14 was carried out on wooden pieces that were used as ribbons between the walls at Kokushikan University in Tokyo by the Japanese Archaeological Mission in Iraq. The result of the test pointed out that the history of the fortress is determined by the year 580 AD plus or minus 90 years. Therefore, the study of the era of the construction of the fortress requires a period of 180 years starting from 490 to 670 AD. This period dates back to the pre-Islamic rule of Iraq more than 140 years and extends to the Umayyad Era. Thus, it is unlikely that the fortress constructed within the Abbasid period[36]. An aerial photograph of the Ukhaidir site was taken in 1935 by KLM British Company (Fig. 2) demonstrated the internal and external walls (sur) and many dwelling houses; it also revealed the presence of water supply channels for the fortress (Kheriz). During the period from 1934 to 1986 AD, many maintenance and excavation campaigns were carried out by the Iraqi Archaeological Foundation inside and outside the fortress[36]. In spite of all these maintenances, the site of Ukhaidir remains neglected and needs urgent maintenance and a large project to preserve the palace's features to prevent it from being affected by the weather conditions, whose effects appeared in most parts of the palace. Excavations that included the digging of several trenches (in the East, Northeast and Northwest) resulted in important discoveries, most notably the appearance of two brick doors, six towers and brick-built walls, in addition to the appearance of complete building units of rooms and facilities built of bricks (seven rooms of different size). Some of the foundations of the walls were built of burnt stones were exposed in the Northern side of the Wadi Al-Abyadh [26].

MATERIALS AND METHODS

Remotely Sensed Dataset

Dual Polarization (HH and HV) of SAR data have been used to extract the information regarding potential archaeological remains in Ukhaidir site, it was a Single Look Complex (SLC) of ALOS PALSAR images (ALOS L1.1), which were being operated during the period 2006–2011 by the Japan Aerospace Exploration Agency (JAXA). The ALOS PALSAR image was acquired on 21 June 2007 [37], with an incident angle of 34.3^0, and a spatial resolution of 12.5 m (intermediate resolution) with 4-8 GHz frequency range and 3.75–7.5 cm wavelength range. SRTM 1 Arc-Second DEM (approximately 30 m) was used to the terrain correction of ALOS PALSAR images. The high-resolution (2 m) Bing satellite image (Fig. 1c) was used as a basemap to test the accuracy of the interpretation, which provides high spatial resolution optical information. Global Digital Surface Model (DSM) "ALOS World 3D – 30 m (AW3D30)" [38] is used to precise 3D map of Ukhaidir site by orthorectification of DSM with Bing satellite image by using ArcScene 10.2 (Fig. 3), where the DSM represents the ground topography of the earth's surface and all objects on it, which considered an elevation model that includes the tops of everything, including buildings, treetops, and ground where there is nothing else on top of it. The digital 3D maps which consist of DSM have been used in various applications, that need to represent land terrains with 5 meters in spatial resolution and 5 meters in height accuracy [39]. In spite of the geometric distortion of the archaeological structure, the map was useful in showing the topography and distinguish the prominent archaeological and hills containing scattered stone surrounding the fortress.

Processing and Interpretation

The processing and interpretation involve the application of three major steps on the ALOS data, Pre-processing, Spatial Texture Analysis (STA) and unsupervised classification (cluster analysis). In this context, the results are evaluated by comparison to optical and historical aerial images as well as field observations.

Pre-Processing

Pre-processing operations include five major processing steps that are applied on the ALOS Level 1.1 using Sentinel Application Platform (SNAP) Software to represent the images as geometrically similar as possible to the real world. These major processing steps are radiometric calibration, multilook, speckle filtering, deskewing and terrain correction, respectively. The radiometric calibration was applied to each intensity band in order to convert the values of the digital number to backscattering coefficient values. Multilooking processing is used to produce a product with a nominal image pixel size, which improves the radiometric resolution of the ALOS image and contain less noise [40]. Speckle filtering is used to reduce the speckles "salt and pepper" from ALOS image thatis caused by random constructive and destructive interference of the de-phased that makes the interpretation more difficult. Deskewing processing will result in adjusting each pixel to a more zero doppler geometry, as well as filling the gaps using digital elevation model (DEM) a type of SRTM 1 Arc-Second. Finally, terrain correction will geocode the image by correcting the distortions of ALOS PALSAR geometric using DEM and producing a projected image (Fig. 4).

Spatial Texture Analysis (STA)

The texture analysis is performed on each band of ALOS image after completing the pre-processing step using gray level co-occurrence matrices (GLCM). The GLCM matrix is considered one of the best statistical matrices used, which was proved strongly in providing vital information from SAR images [41]. In addition, extracting ground features by monitoring land cover, texture measures represent the spatial distribution of the grey-level value and its frequency relative to another one for a specific displacement (x, y) and orientation (0^0, 45^0, 90^0 and 135^0). From a sub-image of a

given window size I (x, y), the GLCM is a matrix P with size GL x GL (GL: the number of gray-levels) whose P (i, j) element ($1 \le i \le GL$; $1 \le j \le GL$) contains the number of times a point with gray-level gi occurs in a set of positions relative (based on the displacement and the angle mentioned before) to another point with gray-level gi[42].The textural features of matrix P are calculated by the following equations:

$$Contrast = \sum_{n=0}^{G_l-1} n^2 \left\{ \sum_{\substack{i=1}}^{G_l} \sum_{\substack{j=1 \\ |i-j|=n}}^{G_l} P(i,j) \right\} \text{..... (1)}$$

$$Dissimilarity = \sum_{i,j=0}^{G_l-1} P_{i,j} \left(-\ln P_{i,j}\right) \text{..... (2)}$$

$$Homogeneity = \sum_i \sum_j \frac{1}{1+(i-j)^2} P(i,j) \text{..... (3)}$$

$$Angular\ Second\ Moment\ (ASM) = \sum_i \sum_j [P\ (i,j)]^2 \text{..... (4)}$$

$$Energy = \sum_{i=0}^{G_L-1} \sum_{j=0}^{G_L-1} P(i,j)^2 \text{..... (5)}$$

$$Entropy = \sum_i P \log\ (P(i,j)) \text{..... (6)}$$

where p (i, j) is the (i, j)-th entry in a normalized grey-tone spatial dependence matrix P(i, j)/R; R is the total sum of P; $p_x(i) = \sum_{j=1}^{G_L} P(i,j)$ is the i-th entry in the marginal probability matrix obtained by summing the rows of p(i, j)[43].

Unsupervised Classification (Cluster Analysis)

Unsupervised classification is considered an effective procedure of dividing remote sensor image and extracting land-cover category based on the spectral signature. Generally, the unsupervised classification employs clustering routines in order to create the number of classes depending on the pixels' similarity, and then assign the identities of the classes after processing. Cluster analysis, also called data segmentation, has a variety of goals, all relating to grouping or collection of objects into clusters, such that those within each cluster are more closely related to one another than objects assigned to different clusters. Among the clustering techniques proposed, K-means technique, which is provided by MacQueen 1967 [44],is considered one of the most prominent statistical analysis techniques. K-means method works to find clusters and cluster centers in a set of unlabeled data. The clustering process is accomplished by reducing distances between objects and the center of the cluster; it requires firstly assigning the number of clusters (k) and iterations. The steps of the algorithm are as follows:

- Identify K centroids for clusters randomly
- Calculate the distance between each point and all centers using the Euclidean distance.

The Euclidean distance is given by the following equation:

$$dij = \sqrt{\sum_{k=1}^{n} (x_{ik} - x_{jk})^2} \text{..... (7)}$$

where$d_{ij}$is theEuclidean distance, n represents thenumber of data points. Then X_{ik}representsthe coordinates of the K property of point i and X_{jk}representthe coordinates of the K property of point j (usually the coordinates of the center).

RESULTS AND DISCUSSION

Among the statistical methods, GLCM considered as a widely used process in many applications to extract the texture features from an image. This method is a square matrix characterizes values of neighboring pixels and describes the relative frequencies depending on the angular relationship between neighboring pixels and on the distance between them. To extract the main features from SAR image, these features must be separated from the background of image by selecting the appropriate displacement angle, window size, quantization level, and the right texture feature [45]. GLCM calculates how often a pixel with gray-level value occurs either horizontally, vertically, or diagonally. Frequently, most of the literatures use all angles to extract the texture features, particularly, in case of unavailability of the ground information and lack of high-resolution image. It is preferable to choose an intermediate window size to suppress noise of SAR image, as applying a small windows size (3x3) may smooth the image too much and result in noisy texture characteristics, whereas increasing windows size (more than 7x7) tends to increase the anisotropy factor [46]. Hence, the choice of the appropriate windowsize is very necessary and depends on the intended application and image resolution. Increasing the quantization level leads to increases in the signal-to-noise ratio. [47,48]. In processing of SAR image, the selection of the quantization level depends on the resolution of the image, when using low quantization level (16 and 32), the anisotropy factor in the image will be higher than when using higher levels. Furthermore, the increases in the number of the quantization level (64, 128, and 256), cause the features to become more pronounced. Although the increasing of levels greatly affects the signal-to-noise ratio.Also, the higher quantization levels tend to focus more in larger structures, whereas the use of lower quantization levels may be more suitable for the interpretation of subtle features [46].

In this work, GLCM used to characterize the textures of ALOS image by applying six common textual features (Contrast, Dissimilarity, Homogeneity, ASM, Energy and entropy), employing all angles (0, 45, 90, 135) with 5x5 window size as shown in the Figure 5. Probabilistic quantizer technique is applied by using a 64-quantization level and one unit of displacement distance to reach the most accurate classification. The analysis of these features exhibit various scattering characteristics. The contrast is the difference in visual perception of the neighboring pixels of the image seen simultaneously or successively. The increase of dissimilarity works linearly instead of increasing exponentially. Contrast gives higher values than does dissimilarity, which is expected since contrast values are larger for every pixel more than one off the diagonal. According to [49], thecontrast and dissimilarity measures pertain to the degree of texture smoothness. The contrast and dissimilarity features (Fig. 5a, 5b) represents the local variations and show the texture fineness in an image, where the coarse texture values are concentrated near the main diagonal, sothey refer to the variation in intensity among neighboring pixels.

A high value of variance indicates a large variation in intensity, which is marked by yellow color and the structures that appear on the surface in addition to the areas where the scattered stone and a texture with low variance has small variation like the barren soil. Homogeneity is one of the important measurement that depicts the local texture feature of image and distinguish different targets [50], it returns a value that measures the closeness of the distribution of elements in the GLCM to the GLCM diagonal. Therefore, it is considered as an indication of how much the texture of image is homogeneous. Figure (5c) point out a homogenous texture in the region with good isolation of anomalies that believed to have different textures. Angular Second Moment (ASM) is the measure of the grey smoothness of the image. High values of ASM occur when image shows coarse texture, as noted in the marked areas(Fig. 5d) and areas where the bricks (scattered stone) are located near the fortress. The energy feature returns to the sum of squared elements in the GLCM matrix, the higher the energy feature value is the more concentrated the distribution of the matrix elements. The results in Figure (5e) show that the increase in energy values reflects the high backscattering values of the targets. The entropy gives a measurement of image randomness content, which describes the image complexity and is considered more suitable to identify the buried or inundated area. The entropy achieves its highest value when the values of GLCM matrix are equal. On the contrary, the inhomogeneous areas have less entropy value [51]. The results (Fig. 5f) reveal that entropy is low in areas with coarse texture, which represent high

backscatter areas and reflecting the non-uniformity of the texture of the image. The textile analysis is identified several potential targets, but the subject has not been definitively resolved. Therefore, a second classification is required. The K-means method is applied, which works to find clusters and cluster centers in a set of unlabeled data. Four of classes (clusters) and five iterations were specified as essential inputs to classifying ALOS image for this study (Fig. 6). The first class represents the barren soil, which has the least spectral signature, and the second class represents the partially covered rocks in the region, while the third and fourth classes represent the uncovered rocks and the archaeological areas. This overlap is due to the fact that the archaeological structures were built from the white valley rocks, which as a result, had a similar spectral signature. The yellow color (class 4) reflects the density of the rock and the structures built in the area. Applying clustering classification, the archaeological structures and uncovered rocks areas put up very strong backscatter; partially covered rocks puts up medium backscatter; barren soil puts up smooth surface and low backscatter. In some areas (west and southwest of fortress), the increase surface roughness of soil (see Figures 1c and 3) caused by scattered stones has led to a high backscatter, while the areas marked with a circuit put up a strong backscatter. It is probable that these areas are likely to be subsurface archaeological remains based on the similarity of their texture with the texture of the fortress.

The results of the two classifications led to the identification of twelve sites, the coordinates of these sites were verified on the field using the application GPS mobile (Fig. 7). Seven sites were excluded because they were uncovered archaeological structures, some of them were clearly visible (see figures 1c and 3) like V1, V2, V3, and V4. Whilst the other three sites (V5, V6 and V7) are diagnosed through field observation in the shape of hills containing scattered stone remains and brick walls. The remaining five sites (P1, P2, P3, P4 and P5) were completely covered with loose sand, their areas are ranging between 873-3774 km^2. P1 and P2 are located northeast of the fortress and P4 and P5 sites in the southwest, while P3 is located about 380 m in the southeast. Potentially, they might be remains of structures for houses or rooms used for military purposes or secret caches connected to the fortress through tunnels. In spite of the discoveries made by the traditional excavations (e.g.-excavated trenches) at Ukhaidir fortress, many excavated sites did not produce any encouraging results [26], which is considered as a major loss of money, effort and time. From our point of view, the results of SAR will be a significant addition to support archaeologists in providing valuable information for documentation of sites and landscapes, the identification of potential areas and management of the future excavation operations.

CONCLUSION

The results of this study show that the potential and the ability of dual polarimetric ALOS PALSAR data to identify the cultural heritage remnants and subsurface archaeological features in the site of Ukhaidir fortress even covered by sand, due to the climate conditions (mainly dry conditions). ALOS L band image represent a non-destructive tool to identify different buried features by analysing backscattering anomaly of the subsurface cultural features, we emphasized significance to exploit in archaeological excavation. The integrated use of the different remote sensing data is an effective and useful tool in the investigation of the buried archaeological structures remains that have an important historical and cultural significance in arid and semi-arid environments, in addition to their low cost compared to traditional methods of archaeological excavation. Although SAR and different remote sensing data cannot substitute ground-based measurements of the traditional methods, it can provide a valuable information of the expected features, and significantly helps to narrows the scope areas of archaeological excavation, especially in large archaeological sites that are difficult to completely excavated.

The approach of using the texture analysis by GLCM and K-Means algorithms allowed a good classification of ALOS image without using the threshold proceedings. The results of GLCM demonstrate well sorted of the anomalies based on the roughness of the texture, whereas K-Means classified the image into four class depending on the intensity of backscattering, and provided better interpretation with supporting of field observations and visual images. However, both of algorithms led to detect both of surface and buried archaeological features. Therefore, the

field observation and the Bing satellite image played an important role in the results of interpretation. The results of the two classification methods yielded to the identification of five anomalies as potential archaeological sites high backscattering values, their areas are ranging between 873-3774 km^2, recommend that they be considered in future excavation operations.

ACKNOWLEDGEMENTS

The authors would like to express their thanks and gratitude to the Japan Aerospace Exploration Agency (JAXA) for providing the ALOS and DSM data as part of the user agreement.

REFERENCES

1. Brivio PA, Pepe M, Tomason R (2000) Multispectral and multiscale remote sensing data for archaeological prospecting in an alpine alluvial plain. J Cult Herit 1:155–164.
2. Wiseman JR, El-Baz F (2007) Remote sensing in archaeology. Springer, New York, NY.
3. Comer D, Harrower M (2013) Mapping Archaeological Landscapes from Space. Springer: New York, NY.
4. Chen F, Masini N, Yang R, Milillo P, Feng D, Lasaponara R (2015) A Space View of Radar Archaeological Marks: First Applications of COSMO-SkyMed X-Band Data. Remote Sens 7:24–50.
5. Gade M, Kohlus J, Kost C (2017) SAR Imaging of Archaeological Sites on Intertidal Flats in the German Wadden Sea. Geosciences 7:105.
6. Tapete D (2018) Remote sensing and geosciences for archaeology. Geosciences 8:41.
7. Elachi C, Roth LE, Schaber GG (1984) Spaceborne radar subsurface imaging in hyperarid regions. IEEE Trans Geosci Remote Sens 22 (4), 383–388.
8. Matzler C (1998) Microwave permittivity of dry sand. IEEE Trans Geosci Remote Sens 36:317–319.
9. Paillou P, Grandjean G, Baghdadi N, Heggy E, August-Bernex T, Achache J (2003) Subsurface imaging in central-southern Egypt using low frequency radar: BirSafsaf revisited. IEEE Trans Geosci Remote Sens 41:1672–1684.
10. Robinson CA, El-Baz F, Al-Saud TS, Jeon SB (2006) Use of radar data to delineate palaeodrainage leading to the Kufra Oasis in the Eastern Sahara. J Afr Earth Sci 44:229–240.
11. Gaber A, Soliman F, Kochc M, El-Baz F (2015) Using full-polarimetric SAR data to characterize the surface sediments in desert areas: A case study in El-Gallaba Plain, Egypt. Remote Sens Environ 162:11–28.
12. Dubois PC, Van Zyl J, Engman T (1995) Measuring soil moisture with imaging radars. IEEE Trans Geosci Remote Sens 33(4): 915–926.
13. Zribi M, Dechambre M (2003) A new empirical model to retrieve soil moisture and roughness from C-band radar data. Remote Sens Environ 84(1): 42–52.
14. Hégarat-Mascl SL, Zribi M, Alem F, Weisse A, Loumagne C (2002) Soil moisture estimation from ERS/SAR data: toward an operational methodology. IEEE Trans Geosci Remote Sens 40(12): 2647-2658.
15. Stewart C (2017) Detection of Archaeological Residues in Vegetated Areas Using Satellite Synthetic Aperture Radar. Remote Sens 9(2): 118.
16. Patel P, Srivastava HS, Panigrahy S, Parihar JS (2006) Comparative evaluation of the sensitivity of multi-polarized multi-frequency SAR backscatter to plant density. Int J Remo Sens 27(2): 293-305.
17. Elachi C, Granger J, (1982) Space-borne imaging radar probe "in depth". IEEE Spectrum 19:24–29.
18. Blom RG, Crippen RE, Elachi C (1984) Detection of subsurface features in Seasat radar images of Means Valley, Mojave Desert, California. Geology 12:346–349.
19. Chen F, You J, Tang P, Zhou W, Masini N, Lasaponara R (2018) Unique performance of spaceborne SAR remote sensing in cultural heritage applications: Overviews and perspectives. ArchaeolProspec 25:71–79.
20. Stewart C, Lasaponara R, Schiavon G (2013) ALOS PALSAR Analysis of the Archaeological Site of Pelusium. ArchaeolProspec 20:109–116.

21. Patruno J, Dore N, Crespi M, Pottier E (2013) PolarimetricMultifrequency and Multi-incidence SAR Sensors Analysis for Archaeological Purposes. ArchaeolProspec 20:89–96.
22. Gaber A, Koch M, Griesh MH, Sato M, El-Baz F (2013) Near-surface imaging of a buried foundation in the Western Desert, Egypt, using space-borne and ground penetrating radar. J ArchaeolSci 40:1946–1955.
23. Dore N, Patruno J, Pottier E, Crespi M (2013) New Research in Polarimetric SAR Technique for Archaeological Purposes using ALOS PALSAR Data. ArchaeolProspec 20:79–87.
24. Chen F, Masini N, Liu J, You J, Lasaponara R (2016) Multi-Frequency Satellite Radar Imaging of Cultural Heritage: The Case Studies of the Yumen Frontier Pass and Niya Ruins in the Western Regions of the Silk Road Corridor. Int J Digit Earth 9:1224–1241.
25. Tapete D, Cigna F (2017) Trends and perspectives of space-borne SAR remote sensing for archaeological landscape and cultural heritage applications. J ArchaeolSci Rep 14:716–726.
26. Al-Hussaini MB (1966) Investigation, Maintenance and Removal of Debris for the Third and Fourth Seasons. Sumer 22:79–94.
27. GETTSSOT (1982) Iraq: A Tourist Guide. General Establishment for Travel and Tourism Services State Organization for Tourism.
28. Francis BY (2017) Encyclopedia of Cities and Sites in Iraq. E-Kutub Ltd.
29. Bell GL (1910) The Vaulting System of Ukhaidir. Journal of Hellenic Studies 30:69–81.
30. Cooper L (2013) Archaeology and Acrimony: Gertrude Bell, Ernst Herzfeld and The Study of Pre-Modern Mesopotamia. Iraq 75:143–169.
31. Hillenbrand R (1994) Islamic Architecture: Form Function and Meaning. New York, Columbia University Press.
32. Bonner J (2017) Islamic Geometric Patterns: Their Historical Development and Traditional Methods of Construction. Springer, New York.
33. Herzfeld E (1910) Die Genesis der islamischenKunst und das Mshatta-Problem, Der Islam 1:105–144.
34. Creswell KA (1958) A Short Account of Early Muslim Architecture. New York, Penguin Books.
35. Bell GL (1914) Palace and Mosque at Ukhaidir: A Study in Early Mohammadan Architecture. Oxford, Clarendon Press.
36. Al-Zaidi AR (2012) Ukhaidir Fortress: A Study in the Light of Investigations, Excavations and Archaeological Maintenance. Al-Ameed Journal 1:539–592.
37. JAXA/METI (2007) ALOS PALSAR L1.1. Accessed through ASF DAAC, [3/2/2017].
38. JAXA (2015) ALOS World 3D – 30m (AW3D30) Version 2.1.
39. JAXA (2017) ALOS Global Digital Surface Model (DSM) "ALOS World 3D-30m" (AW3D30) Dataset: Product Format Description, Version 1.1.
40. ESA (2015) ALOS PALSAR Orthorectification Tutorial.
41. Ulaby FT, Moore RK, Fung AK (1982) Microwave Remote Sensing Active and Passive-Volume II: Radar Remote Sensing and Surface Scattering and Emission Theory. Addison Wesley, Boston, MA.
42. Haralick R, Shanmugan K, Dinstein I (1973) Textural features for image classification. IEEE Trans Syst Man Cybern 3:610–621.
43. Zakeri H, Yamazaki F, Liu W (2017) Texture Analysis and Land Cover Classification of Tehran Using Polarimetric Synthetic Aperture Radar Imagery. ApplSci 7:452.
44. MacQueen JB (1967) Some methods for classification and analysis of multivariate observations. Proceedings of 5-th Berkeley Symposium on Mathematical Statistics and Probability, University of California Press, Berkeley, pp. 281–297.
45. Aghav AS, Narkhede PN (2017) Application-oriented approach to Texture feature extraction using Grey Level Co-occurrence Matrix (GLCM). International Research Journal of Engineering and Technology 4(5):3498- 3503.
46. Eichkitz CG, Amtmann J (2018) GLCM-based anisotropy estimation — the influence of computation parameters on the results. First Break 36:47-52.
47. Chopra S, Alexeev V (2006) Application of texture attribute analysis to 3D seismic data. The Leading Edge 25 (8):934-940.

48. Gao D (2007) Application of three-dimensional seismic texture analysis with special reference to deep-marine facies discrimination and interpretation: Offshore Angola, West Africa. AAPG Bulletin 91(12):1665-1683.
49. Clausi DA, Zhao Y (2002) Rapid extraction of image texture by cooccurrence using a hybrid data structure. ComputGeosci 28(6):763–774
50. Yang K, Cheng Y, Liu J (2011) A Method for Extracting the Text Feature of SAR Image Based on Cooccurence Matrix. Proceedings of 4th International Congress on Image and Signal Processing, Shanghai, pp. 2038-2043.
51. Richards JA (2013) Geometric Processing and Enhancement: Image Domain Techniques. In: Richards JA (ed) Remote Sensing Digital Image Analysis. Springer, Berlin, Heidelberg, pp, 127-159.
52. GCS (1935) General Commission for Survey, Ministry of Water Resources, Iraq.

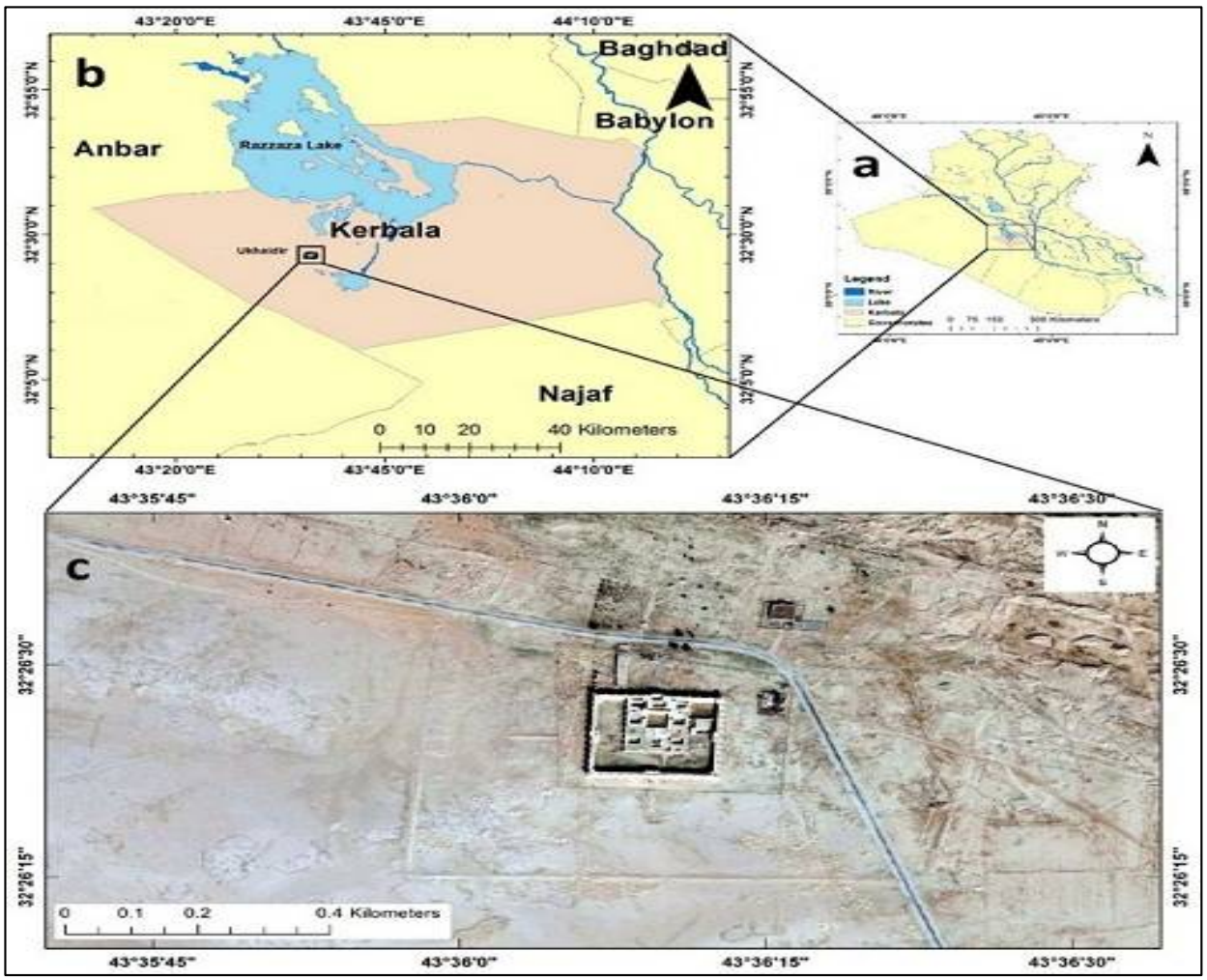

Figure 1. Location of study area: a- Iraq map showing the location of the Karbala Governorate; b- Karbala governorate map showing the location of Ukhaidir fortress; c- High-resolution Bing satellite image of Ukhaidir site

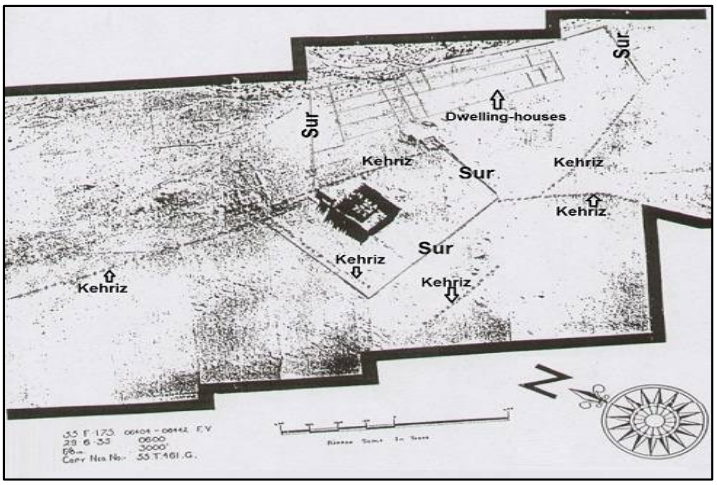

Figure 2. Aerial photograph of the Ukhaidir site demonstrating the internal and external walls (sur), dwelling houses and water channels (Kheriz) [52].

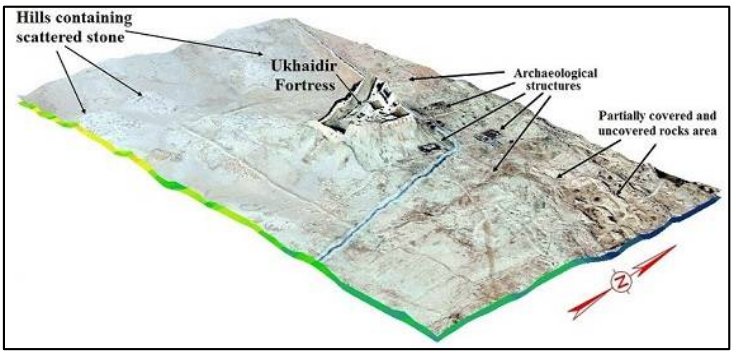

Figure 3. 3D image view illustrates the topography and the landscapes of Ukhaidir site

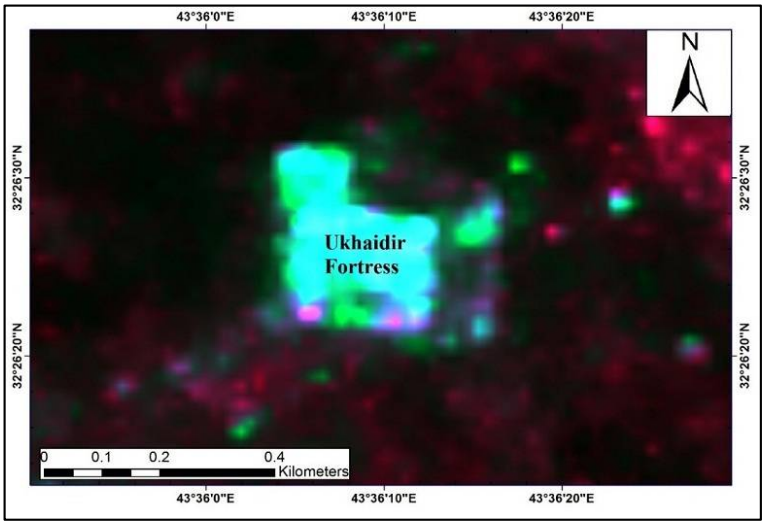

Figure 4. ALOS image after Pre-processing steps, demonstrated the areas that have high backscattering value

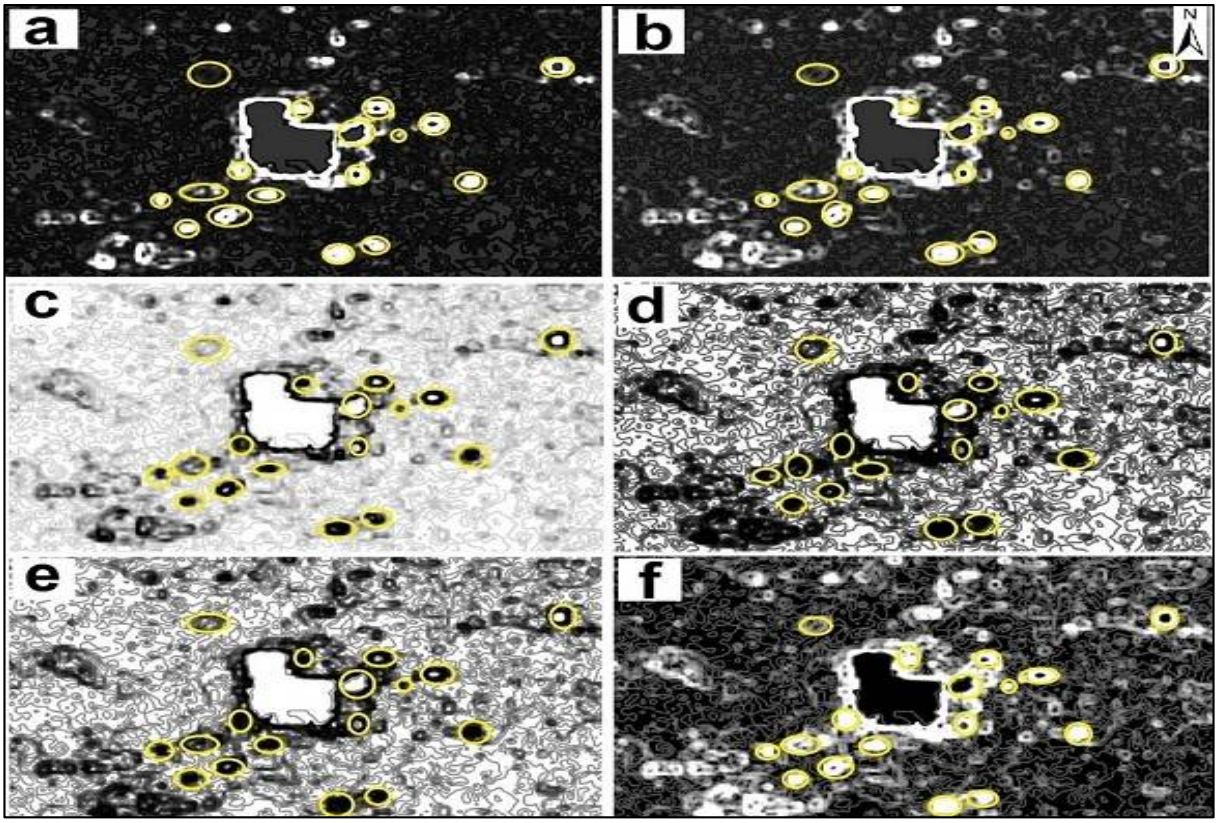

Figure 5. Textual features of GLCM matrix: a- Contrast, b- Dissimilarity, c- Homogeneity, d- ASM, e- Energy and f- Entropy

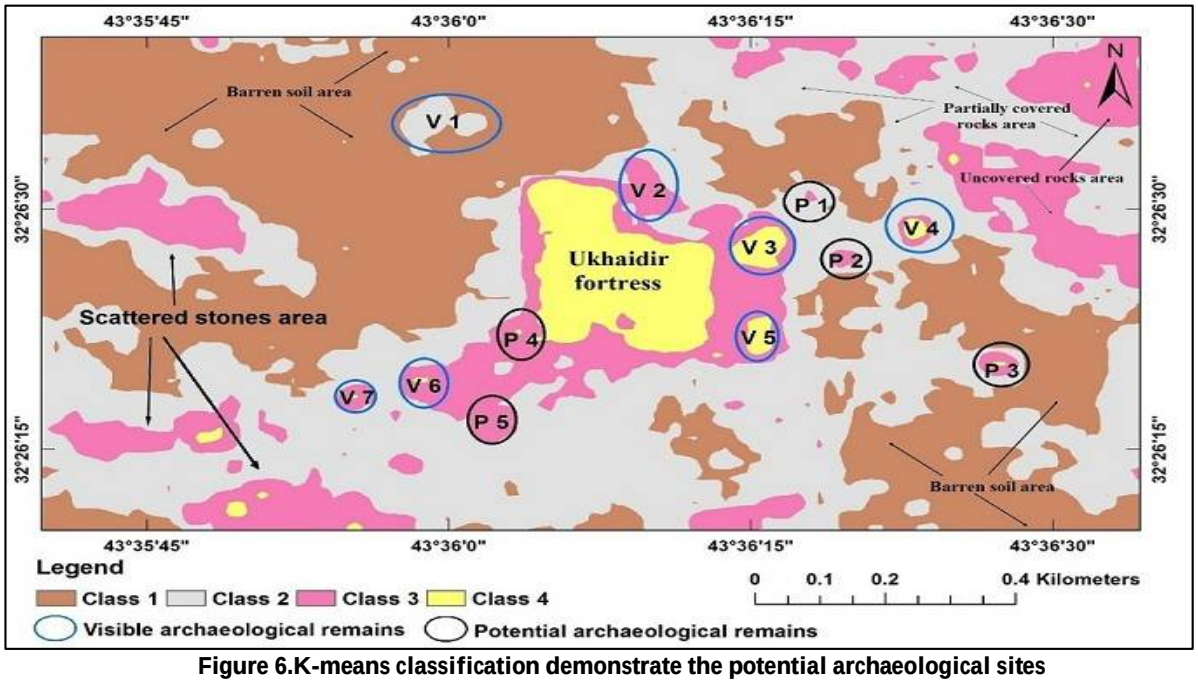

Figure 6.K-means classification demonstrate the potential archaeological sites

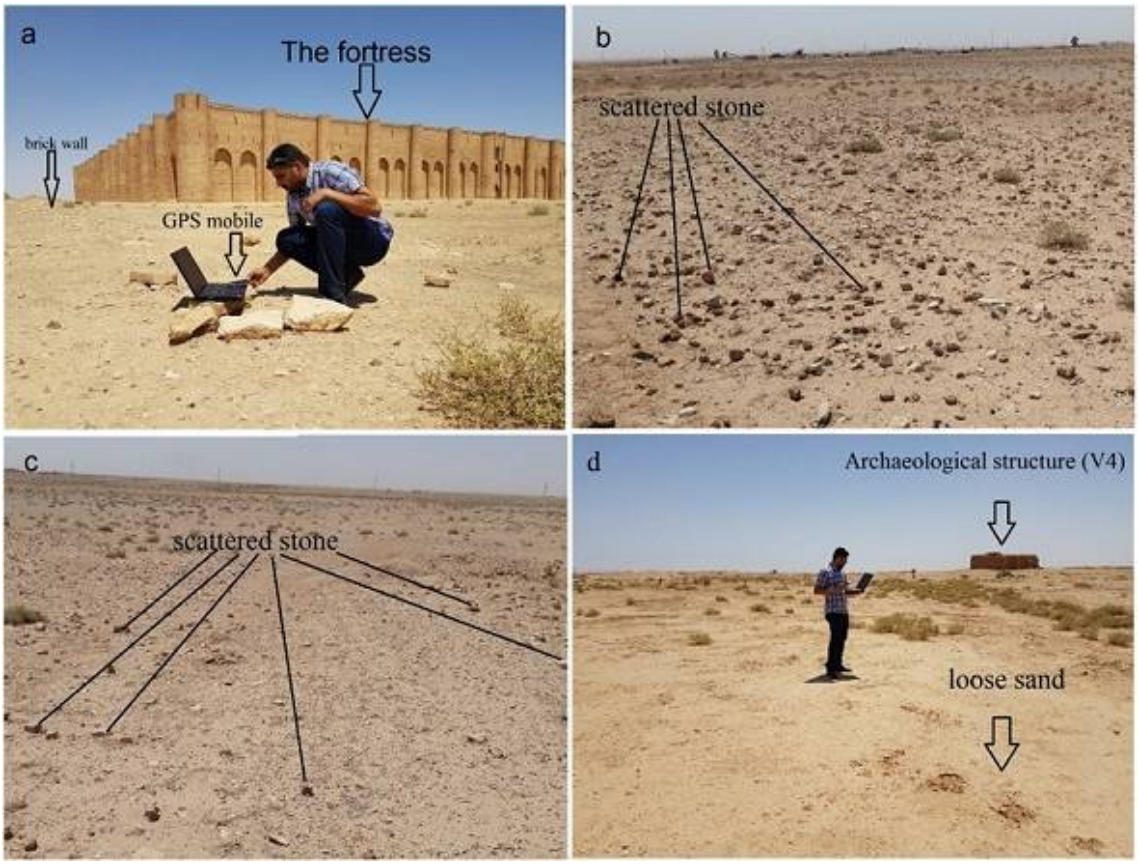

Figure 7. The verification of the coordinates of sites on the field using the application GPS mobile. a- show the brick walls in site V5; b and c- show the scattered stone remains in the site V6 and V7 respectively; d- show the loose sand in site P1 and the archaeological structure in site V4